NJC

PAPER

View Article Online
View Journal



Cite this: DOI: 10.1039/c5nj01684c

# Synthesis, crystal structure, and DNA-binding studies of different coordinate binuclear silver(I) complexes with benzimidazole open-chain ether ligands†

Huilu Wu,* Jiawen Zhang, Chengyong Chen, Han Zhang, Hongping Peng, Fei Wang and Zaihui Yang

Received (in Montpellier, France) 30th June 2015,
Accepted 1st July 2015

DOI: 10.1039/c5nj01684c

www.rsc.org/njc

Three new binuclear silver(I) complexes, namely, $[Ag_2(Meobb)_2](pic)_2{\cdot}2H_2O$ (**1**), $[Ag_2(Etobb)_2(pic)](pic){\cdot}(CH_3CN)$ (**2**) and $[Ag_2(Bobb)_2(pic)_2]$ (**3**) (Meobb = 1,3-bis(1-methylbenzimidazol-2-yl)-2-oxapropane, Etobb = 1,3-bis(1-ethylbenzimidazol-2-yl)-2-oxapropane, Bobb = 1,3-bis(1-benzylbenzimidazol-2-yl)-2-oxapropane, pic = picrate), have been synthesized and characterized by elemental analyses, IR spectroscopy and X-ray single crystal diffraction. Complex **1** displays an $Ag_2(Etobb)_2$ dimeric structure. Each silver(I) ion is coordinated to two nitrogen atoms that adopt a distorted linear configuration. In complex **2**, the coordination environment of silver(I) atoms is different. The Ag1 ion is coordinated in a T-shaped tri-coordinated geometry and the Ag2 is best described to be in a distorted tetrahedron. Complex **3** exhibits a discrete di-silver metallacyclic framework. One silver atom (Ag1) is present in a distorted tetrahedral geometry, whereas the other silver atom (Ag2) is five-coordinated with two nitrogen atoms, oxygen atoms and the Ag1 to form a distorted square-based pyramidal configuration. The interactions of the three complexes with calf thymus DNA (CT-DNA) has been investigated by electronic absorption titration, fluorescence spectroscopy and viscosity measurements, and the modes of CT-DNA binding to the complexes have been proposed. Experimental results suggest that the silver(I) complexes bind to DNA in an intercalation mode, and their binding affinity for DNA follows the order 1 > 2 > 3. The DNA-binding studies demonstrate that steric hindrance has a large influence on the binding ability to DNA. The complex that has smaller steric hindrance binds more strongly to DNA.

## Introduction

In recent decades, the chemistry of silver(I) complexes is an active, thriving field that has attracted a great deal of research interest.[1–4] As more and more silver(I) complexes have been reported, many of them have been used in the fields of luminescence, catalysis, conduction and anticancer agents.[5–8] As a representative $d^{10}$ electronic configurational metal, silver(I) has a very flexible coordination sphere, which enables it to adopt coordination numbers ranging from 2 to 6, even 7 and 8, resulting in coordination geometries varying from linear to T-shaped, tetragonal, square pyramidal and octahedral.[9–11] Another interesting feature of silver(I) is its feasibility to form the short Ag···Ag (argentophilicity), Ag···π and Ag–C interactions in silver(I) coordinated polymers as well as non-covalent supramolecular interactions with aromatic clouds such as π···π, CH···π and anion···π.[12] Moreover, silver(I) has a high affinity towards heteroatoms, like N, O and S, present on the ligands.[13] Thus, more and more ligands containing N and O atoms have been synthesized such as benzimidazoles and their derivatives.

Benzimidazoles and their derivatives have drawn significant attention as an important class of heterocyclic compounds in chemistry and pharmacology.[14–17] Benzimidazole is an important fragment in medicinal chemistry and plays very important roles in numerous pharmaceutically important molecules with a wide range of biological properties. Plenty of compounds containing the benzimidazole group have been reported to exhibit anticancer,[18] antiviral,[19] anti-inflammatory,[20] antimicrobial,[21] antioxidant[22] and anticoagulant properties.[23]

Therefore, the investigation of silver(I) complexes with benzimidazole is becoming a very popular and interesting field. Nowadays, plenty of silver(I) complexes with benzimidazole have been developed and many of them exhibit wide-ranging antimicrobial activity,[24] photoluminescence and catalytic properties[25,26]

*School of Chemical and Biological Engineering, Lanzhou Jiaotong University, Lanzhou, Gansu, 730070, P. R. China. E-mail: wuhuilu@163.com; Fax: +86 13893117544; Tel: +86 13893117544*

† CCDC 721072, 721073 and 1408501. For crystallographic data in CIF or other electronic format see DOI: 10.1039/c5nj01684c

as well as the potential to form supramolecular aggregates through π···π stacking interaction and hydrogen bonding.[27] Based on our previous investigations on silver(I) complexes containing benzimidazole derivatives,[28,29] in this study, we wish to report the synthesis, characterization and DNA-binding activities of silver(I) complexes **1–3** containing three different V-shaped ligands.

## Results and discussion

Synthetic routes towards binuclear silver(I) complexes are exhibited in Scheme 1. The binuclear silver(I) complexes were obtained by the reaction of Ag(pic) with three ligands, namely, Meobb, Etobb and Bobb, in hot methanol. In contrast to silver(I) complexes, the three ligands are stable under atmospheric conditions. The silver(I) complexes are remarkably soluble in polar aprotic solvents such as DMF, DMSO and MeCN; slightly soluble in water, ethanol, methanol, ethyl acetate and chloroform; and insoluble in $Et_2O$ and petroleum ether.

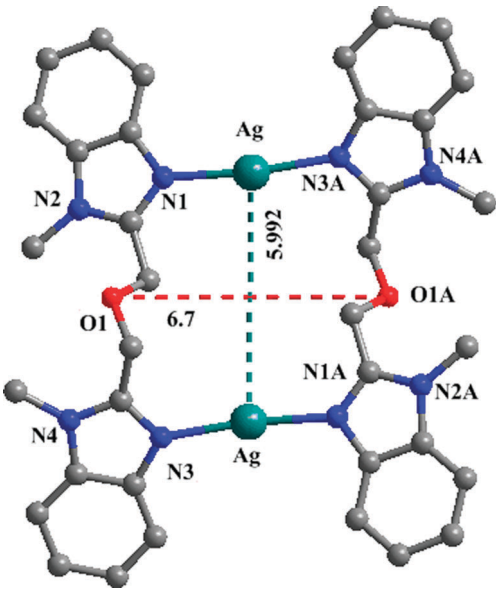


Fig. 1 The molecular structure of **1**; hydrogen atoms and picrate anions are omitted for clarity.

### X-ray structure characterization

The structures of **1**, **2** and **3** are confirmed by X-ray diffraction. The crystal structures are shown in Fig. 1, 3 and 4, respectively.

**Crystal structure of 1.** Crystallographic analysis reveals that complex **1** crystallizes in the triclinic space group $P\bar{1}$, and the structure of complex **1** displays an $M_2L_2$ dimeric structure composed of a dinuclear $[Ag_2(Meobb)_2]^{2+}$ cation, two picrate anions and two aqua molecules. As seen from Fig. 1, two ligands are arranged in an end-to-end fashion to coordinate with two Ag(I) atoms. Each silver(I) ion is coordinated to two nitrogen atoms from two different Meobb ligands, forming a slightly distorted linear $AgN_2$ motif with an N1–Ag–N3 angle of 169.94°. It is noteworthy that this N1–Ag–N3 interaction is the ligand bridge. The $[Ag_2(Meobb)_2]^{2+}$ cation comprises a centrosymmetric binuclear pore canal structure through the N1–Ag–N3 interaction (Fig. 1). The distance of the pore ranges from 5.992 Å ($d_{Ag-Ag}$) to 6.7 Å ($d_{O1-O1A}$). The distance between the two silver(I) centres is 5.992 Å, and is considerably longer than the limit (2.91–3.24 Å) of those reported for weak Ag···Ag interactions in other silver(I)

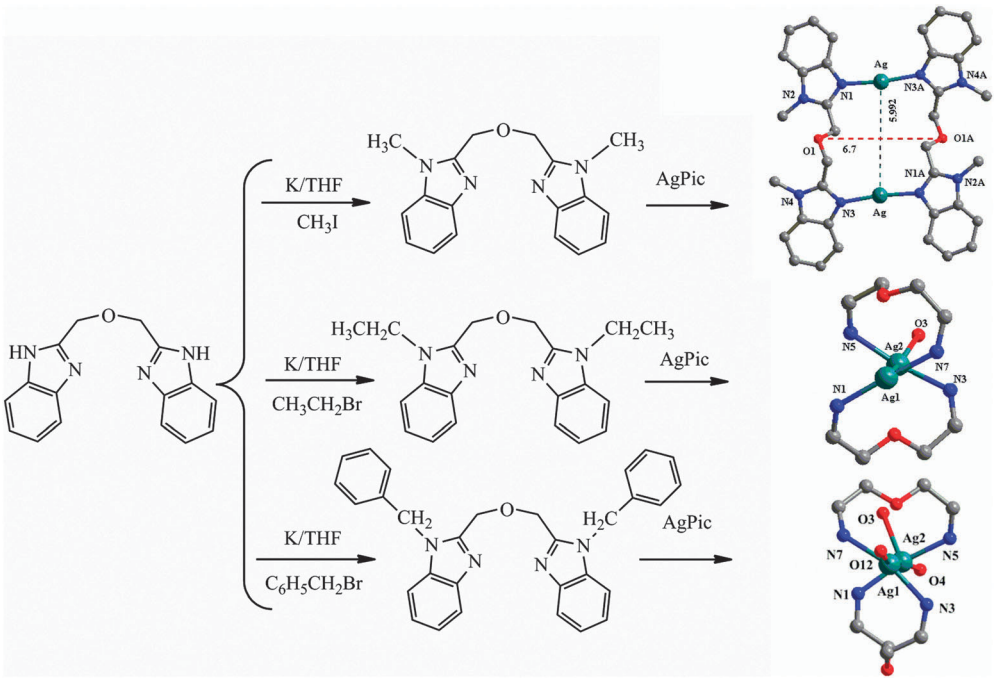


Scheme 1 Synthesis of complexes **1–3**.

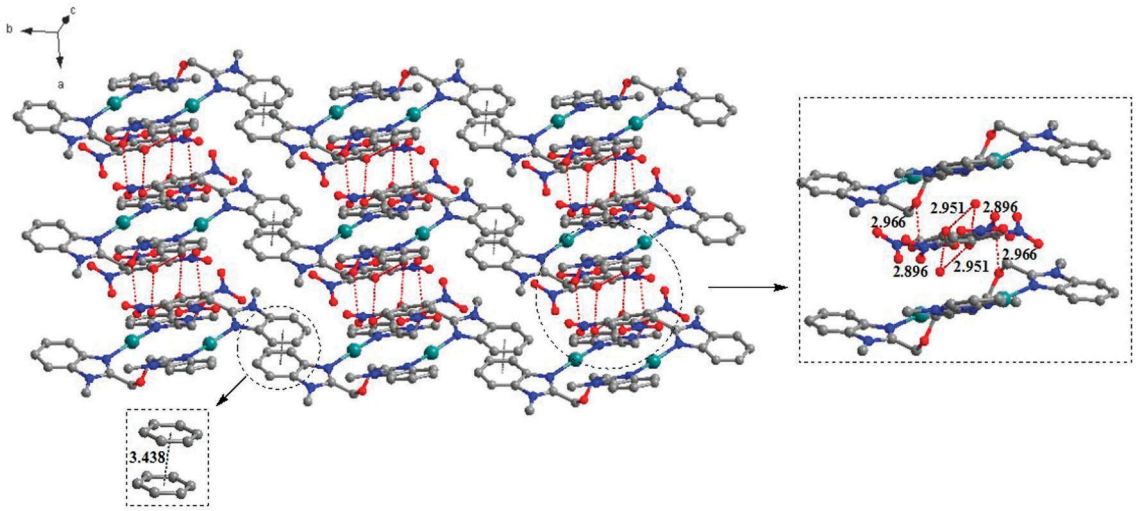


Fig. 2 A view of the packing in complex **1**, showing π···π stacking and hydrogen bonds between neighboring units.

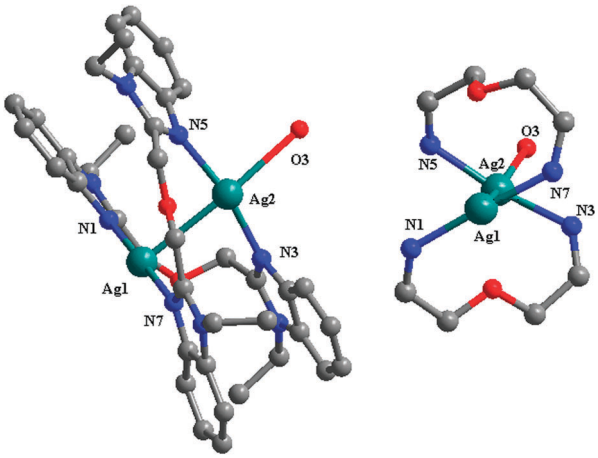


Fig. 3 The cation complex **2** with H-atoms and the uncoordinated picrate anion omitted for clarity (left) and the 8-shaped geometric structure built by two nine-membered rings (right).

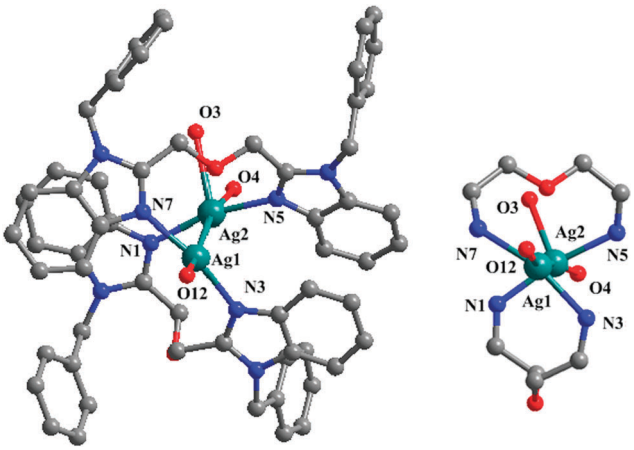


Fig. 4 The neutral unit and atom-labeling scheme of complex **3** (left); hydrogen atoms and solvent molecules are omitted for clarity. The 8-shaped geometric structure of complex **3** (right).

complexes,[30–32] excluding any bonding interactions. It is obvious that the two picrate anions do not participate in the coordination and only act as counter anions for charge equilibrium.

As depicted in Fig. 2, the $[Ag_2(Meobb)_2]^{2+}$ cation in crystalline $[Ag_2(Meobb)_2](pic)_2{\cdot}2H_2O$ stacks through strong π···π interaction between pairs of benzimidazole rings containing N3 and N4 (and symmetry related atoms), extending into a 1-D chain. The distance of the centroid-to-centroid between the two benzimidazole rings is 3.438 Å. This type of interaction plays an important role in stabilization of the framework. It is greatly fascinating that two adjacent picrate anions and two aqua molecules are inlayed in the coordination cations as a sandwich and are connected by hydrogen bonds.

The oxygen atoms of picrate anion and Meobb ligand are the strongest hydrogen bond acceptors, while the O–H groups of hydrone are the strongest hydrogen bond donors in the system.[33] O–H···O hydrogen bonds from hydrogen of O–H to picrate, water and Meobb ligand are shown in the structure of $[Ag_2(Meobb)_2](pic)_2{\cdot}H_2O$ in Fig. 2. Owing to the existence of hydrogen bonds and π···π stacking interaction, an infinite 2-D layer was created.

**Crystal structure of 2.** Single-crystal X-ray diffraction analysis reveals that complex **2** crystallizes in the triclinic space group $P\bar{1}$. The asymmetric unit of **2** is composed of two silver(I) ions, two Etobb ligands and one picrate anion. The average N–Ag bond distance of 2.127 Å is similar to that in $\{[Ag(MeIm)_2](DNB)\}_2{\cdot}H_2O$ (2.1196 Å, MeIm = 2-methylimidazole, DNB = 3,5-dinitrobenzoate),[34] but longer than that in complex **1** (2.106 Å) and shorter than that in complex **3** (2.155 Å). Careful inspection of the crystal structure shows that the two silver(I) ions are coordinated differently; they are three- and four-coordinated (Fig. 3). The coordination geometry around Ag1 ion is best described as T-shaped with the angle of N1–Ag1–N7 as 177.90°. The N3–Ag2–N5 angle (164.91°) is slightly deviated from linearity, but the coordination geometry around Ag2 should be best described to be a distorted tetrahedron considering the O3–Ag2 (2.526 Å) and Ag1–Ag2

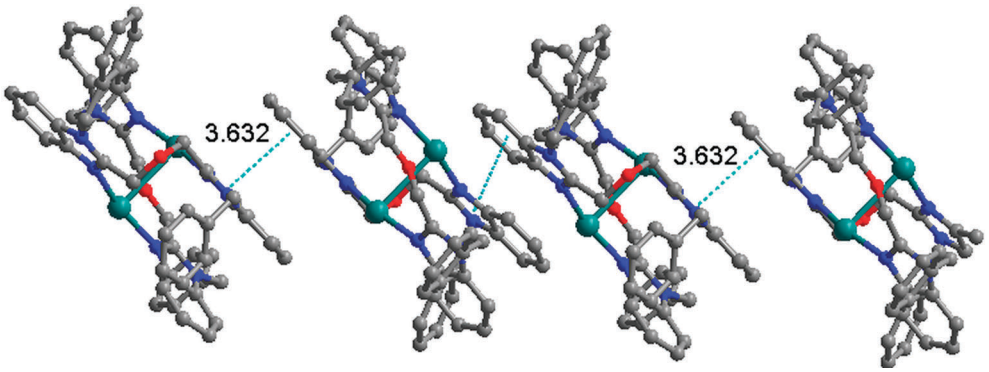


Fig. 5 1-D chain of complex **3** by benzimidazole ring π···π stacking.

(2.997 Å) interactions. The geometry for the four-coordinate transition metal complex can be determined using the $\tau_4$ geometry index, $\tau_4 = [360 - (\alpha + \beta)]/141$, where $\alpha$ and $\beta$ are the largest angles around the metal center.[35] The four coordinate $\tau_4$ values range from one for a perfect tetrahedral geometry to zero for a perfect square planar geometry. The $\tau_4$ parameter for Ag2 is 0.44 and it can be considered to have a slightly distorted seesaw geometry between tetrahedral and square planar. The Ag–Ag contacts lead to dinuclear silver units that are further bridged by the ligand for constructing two nine-membered rings, thus exhibiting an 8-shaped geometry (Fig. 3).

**Crystal structure of 3.** The X-ray structural characterization shows that complex **3** belongs to the triclinic crystal system, crystallizing in the space group $P\bar{1}$. As illustrated in Fig. 4, in complex **3**, the self-assembly of silver(I) ions and ligands gives a dinuclear $[Ag_2(Bobb)_2(pic)_2]$ motif. There are two silver(I) ions that have different coordination environments. The Ag1 ion adopts a distorted tetrahedron coordination geometry ($\tau_4 = [360 - (\alpha + \beta)]/141 = 0.21$; herein, $\alpha$ = N(3)–Ag(1)–N(7) = 163.5° and $\beta$ = O(12)–Ag(1)–Ag(2) = 166.26°) with an oxygen atom (O12) from the picrate group and two nitrogen atoms (N3, N7) from the two chelating Bobb ligands. However, the Ag2 center is five-coordinated with two nitrogen atoms (N5, N1), oxygen atoms (O3, O4) and Ag1 and forms a rarely distorted square-based pyramidal configuration. The parameter ($\tau_5$) of the five-coordinate geometry from a perfect trigonal bipyramidal geometry ($\tau_5 = 1$) towards a regular square-based pyramidal ($\tau_5 = 0$) has been calculated according to the method of Addison *et al.*, $\tau_5 = (\beta - \alpha)/60$, where $\alpha$ and $\beta$ are the largest angles around the metal center.[36] The $\tau_5$ parameter for Ag2 is 0.036 (herein, $\beta$ = O(4)–Ag(2)–Ag(1) = 169.24° and $\alpha$ = N(1)–Ag(2)–N(5) = 167.08°). The Ag1–Ag2 distance is 3.137 Å, which is significantly shorter than the sum of van der Waals radii (3.44 Å), and is rather close to the Ag–Ag distance in silver metal (3.048 Å),[37] indicating the presence of an argentophilic interaction. The average O–Ag bond length of 2.636 Å is longer than that in complex **2** (2.526 Å). The Ag–Ag contacts result in a dinuclear silver unit and are further bridged by the ligand to construct two nine-membered rings, similar to complex **2** (Fig. 3).

As one of the important types of supramolecular forces, π···π stacking shows a specific structural requirement for substrate recognition or for the arrangement of complicated architectures. In complex **3**, the self-assembly of silver(I) ions and Bobb ligands generate infinite 1-D chains, and the asymmetric molecules are connected by π···π stacking interactions from the benzimidazole rings (Fig. 5). The average centroid-to-centroid distance is 3.632 (1) Å.

In summary, three new binuclear silver(I) complexes were synthesized using three ligands Meobb, Etobb and Bobb, respectively, which exhibited diverse intriguing structures. For complex **1**, two Meobb ligands were coordinated with two silver(I) atoms with two N1–Ag–N2 interactions, and each silver(I) ion is two-coordinated. The major structures of complexes **2** and complex **3** are similar and exhibit an 8-shaped geometric structure, but the coordination environment of the silver(I) atoms is different. In complex **2**, the coordination numbers of the two silver(I) atoms are three and four, while the coordination numbers of two silver(I) atoms are four and five in complex **3**. By comparing the molecular structures of the above-mentioned complexes, the reason that the silver(I) complexes exhibit different structural conformation could be ascribed to different distortions and steric hindrance of the ligands.

## DNA-binding studies

**Electronic absorption titration.** DNA-binding is the critical step for DNA cleavage in most cases. The application of electronic absorption spectroscopy in DNA-binding studies is one of the most useful techniques.[38] The binding of metal complexes to DNA helix is often characterized through absorption spectral titration by following the changes in the absorbance and shifts in the wavelength. To clarify the interaction between the complex and DNA, the absorption spectra of **1–3** in the absence and presence of CT-DNA are illustrated in Fig. 6a–c, respectively. These complexes exhibited intense absorption bands at 278–282 nm, ascribed to the π → π* transition of benzimidazole and increasing concentration of CT-DNA. The concentration of CT-DNA affected the absorption most likely through the intercalative mode because intercalation would lead to hypochromism and bathochromism in UV absorption spectra. The intercalative mode involves a strong stacking interaction between an aromatic chromophore and the base pairs of DNA.[39] In the present case, with the addition of DNA, three silver(I) complexes exhibited

 

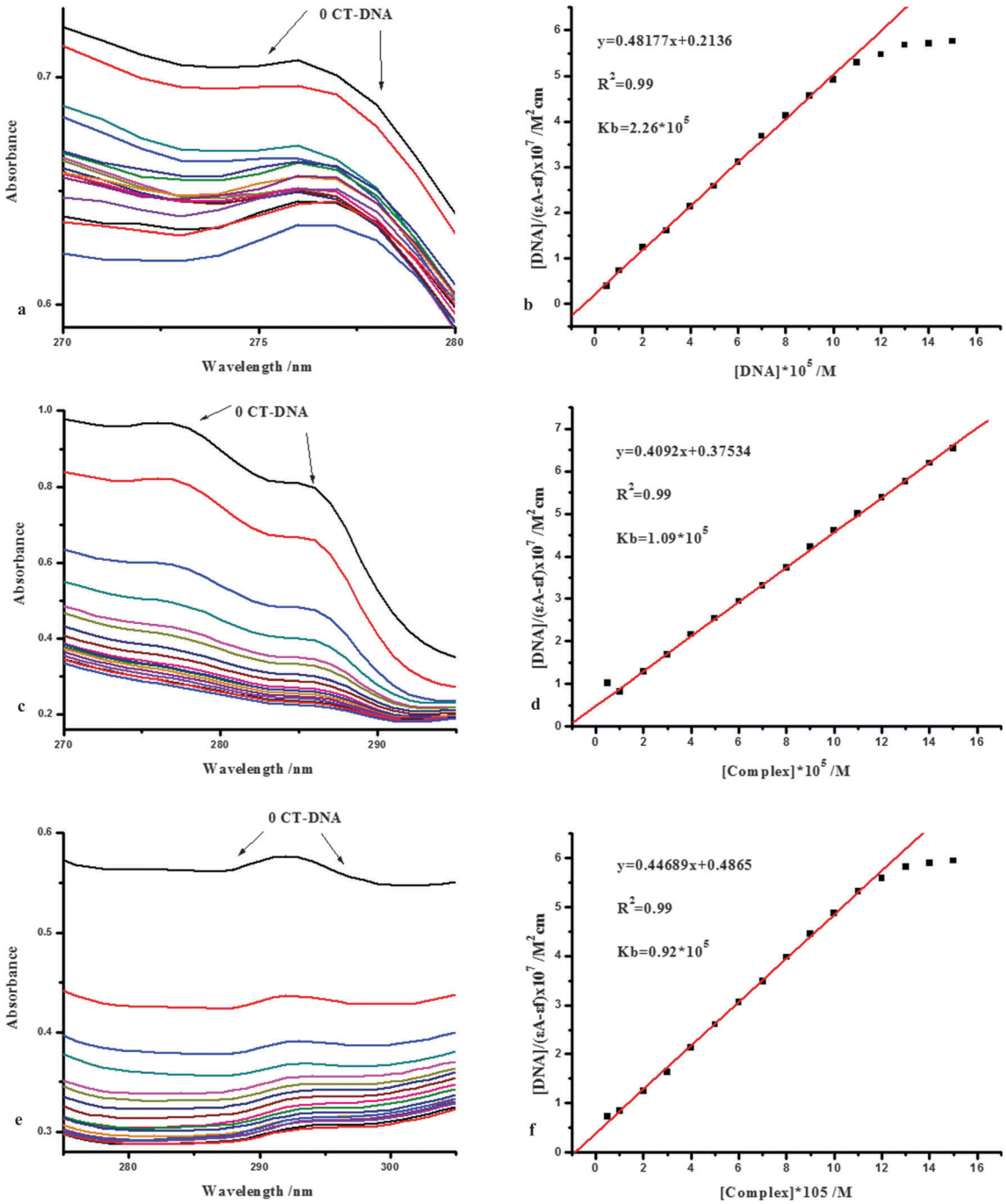


Fig. 6 Absorption spectral traces of (a) complex **1**, (c) complex **2** and (e) complex **3** in Tris-HCl buffer upon the addition of CT-DNA. Arrows show the emission intensity changes upon increasing the DNA concentration. Plots of [DNA]/($\varepsilon_a - \varepsilon_f$) *vs.* [DNA] for the titration of (b) complex **1**, (d) complex **2** and (f) complex **3** with CT-DNA. [complex **1**], [complex **2**] and [complex **3**] = 2.0 × $10^{-5}$ mol $L^{-1}$, [DNA] = 0.5–9.0 × $10^{-5}$ mol $L^{-1}$.

hypochromism of about 10.23%, 72.00% and 46.04%, respectively, accompanied by a bathochromic shift of about 1–2 nm in the absorption maxima. The extent of the hypochromism is consistent with the strength of intercalative interactions.[40]

To compare the affinity of the three Ag(I) complexes towards DNA, the intrinsic binding constants $K_b$ for complexes **1**, **2** and **3** were obtained and are 2.26 × $10^5$ $M^{-1}$ ($R^2$ = 0.99 for 11 points), 1.09 × $10^5$ $M^{-1}$ ($R^2$ = 0.99 for 15 points) and 0.92 × $10^5$ $M^{-1}$ ($R^2$ = 0.99 for 12 points), respectively. The $K_b$ values obtained here are lower than those reported for classical intercalators (for example, ethidium bromide), whose binding constants have been found to be $10^6$ $M^{-1}$ [41] and is three orders of magnitude more than our previous investigation on silver(I) complexes containing benzimidazole derivatives.[29] These results indicate that there is an intercalative binding mode between the three complexes and CT-DNA. As can been seen from Fig. 6, the binding

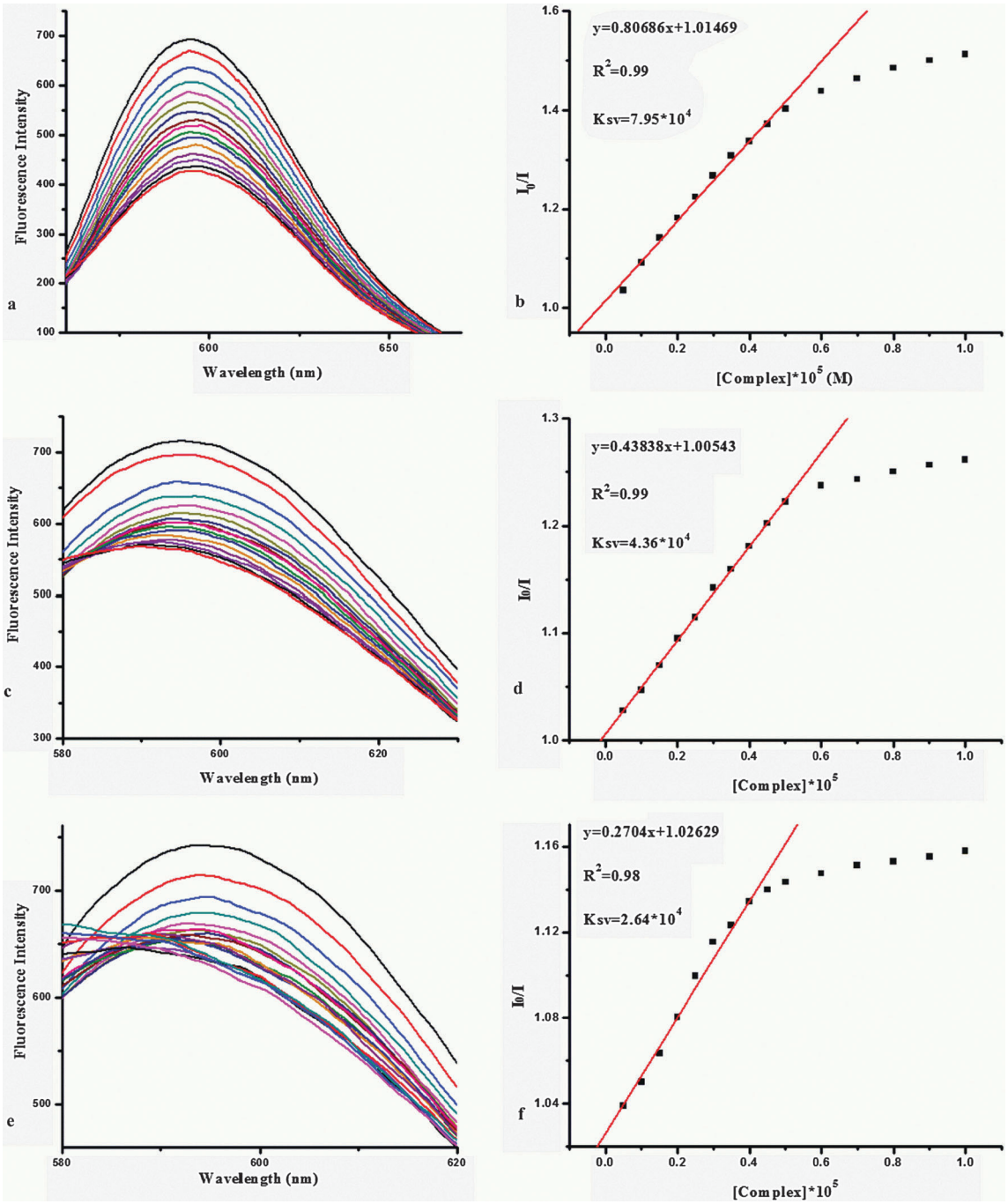


Fig. 7 Emission spectra of EB bound to DNA in the presence of (a) complex **1**, (c) complex **2** and (e) complex **3** in Tris-HCl buffer. Fluorescence quenching curves of EB bound to CT-DNA by (b) complex **1**, (d) complex **2** and (f) complex **3**. (Plots of $I_0/I$ *vs.* [complex]). [DNA] = 2.5 × $10^{-3}$ mol $L^{-1}$; $\lambda_{ex}$ = 520 nm.

strengths of the complexes follow the order 1 > 2 > 3. The reason for the difference in the binding strengths of these three Ag(I) complexes can be attributed to the difference in steric hindrance, which is caused by both the introduction of substituents and geometric structure.

**Fluorescence spectroscopic studies.** No luminescence was observed for complexes **1–3** at room temperature either in DMF or in the presence of CT-DNA. The binding of the complexes cannot be directly followed in the emission spectra. Therefore, steady state competitive binding studies of the three complexes were monitored by a fluorescent EB displacement assay. EB is a planar aromatic heterocyclic dye that intercalates non-specifically into the DNA and causes it to fluoresce strongly.[42,43]

EB (weak fluorescence) + DNA (no fluorescence) ↔
EB-DNA (strong fluorescence)

Thus, EB can be used to probe the interaction of the complexes with DNA. The relative binding of the complexes **1–3** to CT-DNA is studied with an EB-bound CT-DNA solution in 5 mM

 

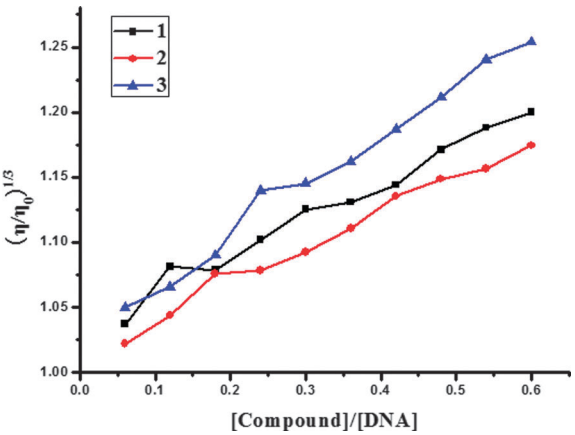


Fig. 8 Effect of increasing amounts of the complexes on the relative viscosity of CT-DNA at 25.0 ± 0.1 °C.

Tris-HCl/50 mM NaCl buffer (pH = 7.2), as shown in Fig. 7. Fluorescence intensities (520 nm excitation) are measured at different complex concentrations. The emission intensity of the DNA–EB system decreases appreciably, which indicated that the complexes could replace EB from the DNA–EB system. Such a characteristic change is often observed in intercalative binding modes.[44] As shown in Fig. 7, the quenching plot illustrates that the quenching of EB bound to DNA by complex is in agreement with the Stern–Volmer relationship, which also indicates the complex binding to DNA. The $K_{sv}$ values for complexes **1–3** are found to be $7.95 \times 10^4$ ($R^2$ = 0.99 for 10 points), $4.36 \times 10^4$ ($R^2$ = 0.99 for 10 points) and $2.64 \times 10^4$ ($R^2$ = 0.98 for 8 points), respectively. The Stern–Volmer dynamic quenching constants can also be interpreted as binding affinities of the complexation reaction.[45,46] The $K_{sv}$ values obtained here are similar to our previous study on silver(I) complexes containing benzimidazole derivatives.[28] Moreover, the binding ability to CT-DNA follows the order 1 > 2 > 3. The results we obtained from the fluorescence spectra are the same as those from absorption spectra.

**Viscosity measurements.** Hydrodynamic measurements that are sensitive to changes in DNA length are considered as the least ambiguous and most critical tests for a binding model in solution in the absence of crystallographic data.[47] To further investigate the interaction properties between the metal complexes and DNA, the relative specific viscosity of DNA was examined by varying the concentration of the added metal complexes. Measuring the viscosity of DNA is a classical technique used to analyze the DNA binding mode in solution.[48] A classical intercalative mode causes significant increases in the viscosity of the DNA solution due to an increase in the separation of base pairs at the intercalation sites, and hence an increase in overall DNA length. In contrast, the complexes those bind in DNA grooves by partial and/or non-classical intercalation cause less pronounced (positive or negative) or no change in DNA solution viscosity.[49] Fig. 8 depicts the effect of complexes **1–3** on DNA viscosity. These results reveal that complex **1**, **2** and **3** produce a relatively apparent increase in DNA viscosity, which is consistent with DNA intercalative binding modes suggested above.[50] These results support the fact that the complexes **1–3** bind to CT-DNA through intercalation.[51]

# Conclusions

In this study, three benzimidazole open-chain ether ligands and their silver(I) complexes have been synthesized and characterized. In complexes **1–3**, all the benzimidazole ligands adopt the $\mu_2$-bridging mode to link two silver atoms, forming three different binuclear motifs. Complex **2** and **3** display an obvious Ag–Ag contact. DNA-binding of the Ag(I) complexes suggest that the three Ag(I) complexes bind to DNA through an intercalation mode owing to the large planar aromatic rings, hydrogen bonds and π···π stacking interactions, which facilitate their intercalation into the base pairs of double helical DNA. Furthermore, the binding affinities of these Ag(I) complexes follow the order **1** > **2** > **3**. This result illustrates that steric hindrance plays a vital role in the DNA-binding of the three Ag(I) complexes. These studies suggest that Ag(I) complexes have potential practical applications in the development of probes for DNA structure and conformations, as well as new therapeutic reagents for diseases on the molecular level, thus warranting further *in vivo* experiments and pharmacological assays.

# Experimental

***Caution***: Although no problems were encountered in this study, transition-metal picrate salts are potentially explosive and thus should be prepared in small quantities and handled with care.

### Materials and instrumentation

The Meobb, Etobb and Bobb ligands were synthesized according to the procedure given in ref. 52. Ethidium bromide (EB) and calf thymus DNA (CT-DNA) were purchased from Sigma Chemicals Co. (USA). Tris-HCl buffer solution was prepared using double-distilled water.

CHN elemental analyses were performed using a Carlo Erba 1106 elemental analyzer. IR spectra were recorded in the 4000–400 $cm^{-1}$ region with a Nicolet FT-VERTEX 70 spectrophotometer using KBr pellets. The electronic spectra were obtained on a Lab-Tech UV Bluestar spectrophotometer. Fluorescence spectral data were obtained on a 970-CRT fluorescence spectrophotometer at room temperature.

### Synthesis

All three complexes were prepared using a similar procedure. The ligand (0.50 mmol: Meobb, 153 mg; Etobb, 167 mg; Bobb, 229 mg) in hot MeOH (15 mL) was added to silver(I) picrate (0.25 mmol, 84 mg) in MeOH (5 mL). A colorless crystalline product was formed rapidly. The precipitate was filtered-off, washed with MeOH and absolute $Et_2O$, and dried *in vacuo*. The product was dissolved in MeCN to obtain a colorless solution that was allowed to evaporate at room temperature. Colorless crystals suitable for X-ray diffraction studies were obtained after several days.

**Complex 1.** Yield 71%. Anal. calcd for $C_{48}H_{44}Ag_2N_{14}O_{18}$ (%): C, 43.61; H, 3.33; N, 14.84. Found (%): C, 44.02; H, 3.35; N, 14.89. Selected IR data (KBr, $\nu/cm^{-1}$), 1084 ($\nu_{C-O-C}$), 1330 ($\nu_{NO_2}$), 1492 ($\nu_{C=N-C=C}$).

**Complex 2.** Yield 67%. Anal. calcd for $C_{54}H_{51}Ag_2N_{15}O_{16}$ (%): C, 46.89; H, 3.69; N, 15.20. Found (%): C, 46.85; H, 3.71; N, 15.18. Selected IR data (KBr, $\nu$/cm$^{-1}$), 1078 ($\nu_{C-O-C}$), 1330 ($\nu_{NO_2}$), 1483 ($\nu_{C=N-C=C}$).

**Complex 3.** Yield 71%. Anal. calcd for $C_{72}H_{56}Ag_2N_{14}O_{16}$ (%): C, 54.37; H, 3.52; N, 12.33. Found (%): C, 54.35; H, 3.61; N, 12.14. Selected IR data (KBr, $\nu$/cm$^{-1}$), 1068 ($\nu_{C-O-C}$), 1330 ($\nu_{NO_2}$), 1471 ($\nu_{C=N-C=C}$).

## X-ray diffraction

For each complex, a suitable single crystal was mounted on glass fibers for data collection in a Bruker Smart CCD diffractometer with graphite-monochromated Mo-Kα radiation ($\lambda$ = 0.71073 Å) at 153 K. Data reduction and cell refinement were performed using the SMART and SAINT programs.[53] The absorption corrections were carried out by the empirical method. The structure was solved by direct methods and refined by a full-matrix of least-squares against $F^2$ for data using the SHELXTL software.[54] All H atoms were found in difference electron maps and were subsequently refined in a riding-model approximation with C–H distances ranging from 0.95 to 0.99 Å. Information concerning the crystallographic data collection and structural refinements is summarized in Table 1. The relevant bond lengths and angles are listed in Table 2.

CCDC reference numbers are 721073, 721072 and 1408501, respectively.

## DNA-binding studies

**Electronic absorption spectra.** The DNA-binding experiments were carried out at room temperature. Using the electronic absorption spectral method, the relative bindings of the three complexes to CT-DNA were studied in 5 mM Tris-HCl/50 mM NaCl buffer (pH = 7.2). The solution of CT-DNA gave a ratio of UV absorbance at 260 nm and 280 nm, $A_{260}/A_{280}$, of 1.8–1.9, indicating that the DNA is sufficiently free of protein.[55] The CT-DNA stock solutions were prepared in 5 mM Tris-HCl/50 mM NaCl buffer, pH = 7.2 (CT-DNA stock solutions were stored at 4 °C and used within 4 days after preparation). The concentration

Table 2 The relevant bond distances (Å) and angles (°) for complexes **1–3**[a]

| | | | |
|---|---|---|---|
| Complex **1** | | | |
| Ag–N(1) | 2.1088(16) | N(3)–Ag#1 | 2.1038(15) |
| Ag–N(3)#1 | 2.1038(15) | | |
| C(9)–O(1)–C(8) | 112.12(14) | C(1)–N(1)–Ag | 123.11(13) |
| N(3)#1–Ag–N(1) | 169.94(6) | C(7)–N(1)–Ag | 129.50(13) |
| C(10)–N(3)–Ag#1 | 126.54(13) | C(16)–N(3)–Ag#1 | 126.57(13) |
| Complex **2** | | | |
| Ag(1)–N(1) | 2.124(3) | Ag(1)–N(7) | 2.134(3) |
| Ag(1)–Ag(2) | 2.9973(4) | Ag(2)–N(3) | 2.117(3) |
| Ag(2)–N(5) | 2.134(3) | Ag(2)–O(3) | 2.526(3) |
| N(1)–Ag(1)–N(7) | 177.90(12) | N(1)–Ag(1)–Ag(2) | 90.66(8) |
| N(7)–Ag(1)–Ag(2) | 89.32(8) | N(3)–Ag(2)–N(5) | 164.91(12) |
| N(3)–Ag(2)–O(3) | 104.34(12) | N(5)–Ag(2)–O(3) | 90.63(12) |
| N(3)–Ag(2)–Ag(1) | 79.32(8) | N(5)–Ag(2)–Ag(1) | 89.23(8) |
| O(3)–Ag(2)–Ag(1) | 132.51(7) | C(41)–O(3)–Ag(2) | 141.5(3) |
| Complex **3** | | | |
| Ag(1)–N(3) | 2.166(5) | Ag(1)–N(7) | 2.174(5) |
| Ag(1)–O(12) | 2.551(4) | Ag(1)–Ag(2) | 3.1365(7) |
| Ag(2)–N(1) | 2.138(5) | Ag(2)–N(5) | 2.145(5) |
| N(3)–Ag(1)–N(7) | 163.5(2) | N(3)–Ag(1)–O(12) | 103.15(17) |
| N(7)–Ag(1)–O(12) | 85.46(18) | N(3)–Ag(1)–Ag(2) | 86.16(13) |
| N(7)–Ag(1)–Ag(2) | 88.14(14) | O(12)–Ag(1)–Ag(2) | 166.26(10) |
| N(1)–Ag(2)–N(5) | 167.08(19) | N(1)–Ag(2)–Ag(1) | 83.42(14) |
| N(5)–Ag(2)–Ag(1) | 88.90(14) | C(68)–O(12)–Ag(1) | 124.3(4) |

[a] Symmetry transformations used to generate equivalent atoms: #1 1 − $x$, 1 − $y$, −$z$.

Table 1 Crystallographic data and structural refinement parameters for complexes **1–3**

| Complex | **1** | 2 | 3 |
|---|---|---|---|
| Empirical formula | $C_{48}H_{44}Ag_2N_{14}O_{18}$ | $C_{54}H_{51}Ag_2N_{15}O_{16}$ | $C_{72}H_{56}Ag_2N_{14}O_{16}$ |
| Mr | 1320.71 | 1381.84 | 1589.05 |
| Crystal system | Triclinic | Triclinic | Triclinic |
| Space group | $P\bar{1}$ | $P\bar{1}$ | $P\bar{1}$ |
| $a$ (Å) | 7.09520(10) | 11.7172(3) | 13.3730(3) |
| $b$ (Å) | 12.8978(3) | 11.9846(3) | 14.8244(4) |
| $c$ (Å) | 15.0574(4) | 20.1196(6) | 17.3282(4) |
| $\alpha$ (°) | 110.5830(10) | 89.9760(10) | 86.8670(10) |
| $\beta$ (°) | 102.7630(10) | 81.0430(10) | 89.7150(10) |
| $\gamma$ (°) | 97.5890(10) | 79.8740(10) | 87.8750(10) |
| $V$ (Å$^3$) | 1224.46(5) | 2746.33(13) | 3427.75(14) |
| $Z$, Dc (mg m$^{-3}$) | 1, 1.791 | 2, 1.671 | 2, 1.540 |
| $\mu$ (mm$^{-1}$) | 0.895 | 0.800 | 0.652 |
| $F$(000) | 668 | 1404 | 1616 |
| $\theta$ Range (°) | 3.02–27.48 | 3.00–27.48 | 3.04–25.50 |
| Limiting indices, $hkl$ | −8 to 9 | −15 to 13 | −16 to 16 |
| | −16 to 16 | −15 to 15 | −17 to 17 |
| | −19 to 19 | −26 to 26 | −20 to 20 |
| Reflections collected | 12 128 | 26 608 | 28 124 |
| Unique reflections | 5602 | 12 603 | 12 762 |
| $R_{int}$ | 0.0151 | 0.0350 | 0.0352 |
| Goodness-of-fit on $F^2$ | 1.031 | 1.062 | 1.179 |
| $R1$/w$R2$ [$I > 2\sigma(I)$] | 0.0223/0.0731 | 0.0390/0.1120 | 0.0487/0.1228 |
| $R1$/w$R2$ (all data) | 0.0245/0.0781 | 0.0534/0.1248 | 0.0877/0.1900 |
| Largest diff. peak, hole (e Å$^{-3}$) | 0.519, −0.582 | 0.729, −0.950 | 1.618, −1.531 |

 

of CT-DNA was determined from its absorption intensity at 260 nm with a molar extinction coefficient of 6600 $M^{-1}$ $cm^{-1}$.[56]

Absorption titration experiments were performed with fixed concentrations of the complexes (25 μL) while gradually increasing the concentration of DNA. When measuring the absorption spectra, an equal amount of DNA was added to both complex solution (2.5 mL Tris-HCl + 25 μL complexes solution) and the reference solution (2.5 mL Tris-HCl + 25 μL DMF) to eliminate the absorbance of DNA itself. The solutions were allowed to incubate for 5 min before the absorption spectra was recorded. The titration processes were repeated until there was no change in the spectra, indicating that binding saturation had been achieved ([complex] = $2.00 \times 10^{-3}$ mol $L^{-1}$). From the absorption titration data, the binding constant ($K_b$) was calculated using the following equation:[39]

$$[DNA]/(\varepsilon_a - \varepsilon_f) = [DNA]/(\varepsilon_b - \varepsilon_f) + 1/K_b(\varepsilon_b - \varepsilon_f)$$

Herein, [DNA] is the concentration of CT-DNA in base pairs, $\varepsilon_a$ corresponds to the extinction coefficient observed ($A_{obsd}/[M]$), $\varepsilon_f$ corresponds to the extinction coefficient of the free compound, $\varepsilon_b$ is the extinction coefficient of the compound when fully bound to CT-DNA, and $K_b$ is the intrinsic binding constant. The ratio of the slope to the intercept in the plot of $[DNA]/(\varepsilon_a - \varepsilon_f)$ *versus* [DNA] gives the values of $K_b$.

**Fluorescence spectra.** A competitive binding of the complex to CT-DNA led to the displacement of bound EB or quenching of bound EB, and as a consequence the emission intensity of ethidium bromide decreased. To further investigate the binding properties of the complex with DNA, competitive binding experiments were performed. The competitive binding experiments were carried out in the buffer by keeping [DNA]/[EB] = 1.14 ([CT-DNA] = $2.50 \times 10^{-3}$ mol $L^{-1}$, [EB] = $2.20 \times 10^{-3}$ mol $L^{-1}$) and altering the concentration of the complexes. The fluorescence spectra of EB were measured using an excitation wavelength of 520 nm and the emission range was set between 550 and 750 nm. The spectra were analyzed based on the classical Stern–Volmer equation[57]:

$$I_0/I = 1 + K_{sv}[Q]$$

Herein, $I_0$ and $I$ are the fluorescence intensities at 599 nm in the absence and presence of the quencher, respectively, $K_{sv}$ is the linear Stern–Volmer quenching constant, and $[Q]$ is the concentration of the complexes. In these experiments, [CT-DNA] = $2.5 \times 10^{-3}$ mol $L^{-1}$ and [EB] = $2.2 \times 10^{-3}$ mol $L^{-1}$.

**Viscosity experiments.** Viscosity measurements were carried out on an Ubbelohde viscometer immersed in a thermostatic water-bath maintained at a constant temperature of 25.0 ± 0.1 °C. Titrations were performed for the complexes (3 mM), and each complex was introduced into a CT-DNA solution (50 μM) present in the viscometer. Data was presented as $(\eta/\eta_0)^{1/3}$ *versus* the ratio of the concentration of the complex to CT-DNA, where $\eta$ was the viscosity of CT-DNA in the presence of the complex and $\eta_0$ is the viscosity of CT-DNA alone. Viscosity values have been calculated from the observed flow time of the CT-DNA containing solution and corrected from the flow time of buffer alone ($t_0$), $\eta = (t - t_0)/t_0$.[58]

## Acknowledgements

The present research was supported by the National Natural Science Foundation of China (Grant No. 21367017) and the Natural Science Foundation of Gansu Province (Grant No. 1212RJZA037).

## References

1 J. J. Perry, J. A. Perman and M. J. Zaworotko, *Chem. Soc. Rev.*, 2009, **38**, 1400–1417.
2 N. C. Kasuga, A. Sugie and K. Nomiya, *Dalton Trans.*, 2004, 3732–3740.
3 B. Moulton, J. J. Lu, R. Hajndl, S. Hariharan and M. J. Zaworotko, *Angew. Chem., Int. Ed.*, 2002, **41**, 2821–2824.
4 D. Sun, N. Zhang, Q. J. Xu, Z. H. Wei, R. B. Huang and L. S. Zheng, *Inorg. Chim. Acta*, 2011, **368**, 67–73.
5 L. Hou and D. Li, *Inorg. Chem. Commun.*, 2005, **8**, 128–130.
6 Y. Cui and C. He, *J. Am. Chem. Soc.*, 2003, **125**, 16202–16203.
7 D. Sun, C. F. Yang, H. R. Xu, H. X. Zhao, Z. H. Wei, N. Zhang, L. J. Yu, R. B. Huang and L. S. Zheng, *Chem. Commun.*, 2010, **46**, 8168–8170.
8 M. A. Fik, A. Gorczynski, M. Kubicki, Z. Hnatejko, A. Fedoruk-Wyszomirska, E. Wyszko, M. Giel-Pietraszuk and V. Patroniak, *Eur. J. Med. Chem.*, 2014, **86**, 456–468.
9 X. F. Zheng and L. G. Zhu, *Inorg. Chim. Acta*, 2011, **365**, 419–429.
10 D. Venkataraman, Y. H. Du, S. R. Wilson, K. A. Hirsch, P. Zhang and J. S. Moore, *J. Chem. Educ.*, 1997, **74**(8), 915.
11 F. A. Cotton and G. Wilkinson, *Adv. Inorg. Chem.*, Wiley, Chichester, 5th ed, 1988.
12 K. Chainok, S. M. Neville, C. M. Forsyth, W. J. Gee, K. S. Murray and S. R. Batten, *CrystEngComm*, 2012, **14**, 3717–3726.
13 G. K. Kole, C. K. Chin, G. K. Tan and J. J. Vittal, *Polyhedron*, 2013, **52**, 1440–1448.
14 M. Boiani and M. González, *Mini-Rev. Med. Chem.*, 2005, **5**, 409–424.
15 A. Ahmed, E. Rashedy, Y. Hassan and A. Enein, *Curr. Drug Ther.*, 2013, **8**, 1–14.
16 K. Kubo, Y. Kohara, Y. Yoshimura, Y. Inada, Y. Shibouta, Y. Furukawa, T. Kato, K. Nishikawa and T. Naka, *J. Med. Chem.*, 1993, **36**(16), 2343–2349.
17 R. C. Boruah and E. B. Skibo, *J. Med. Chem.*, 1994, **37**(11), 1625–1631.
18 Y. S. Tong, J. J. Bouska, P. A. Ellis, E. F. Johnson, J. Leverson, X. S. Liu, P. A. Marcotte, A. M. Olson, D. J. Osterling, M. Przytulinska, L. E. Rodriguez, Y. Shi, N. Soni, J. Stavropoulos, S. Thomas, C. K. Donawho, D. J. Frost, Y. Luo, V. L. Giranda and T. D. Penning, *J. Med. Chem.*, 2009, **52**(21), 6803–6813.
19 Y. F. Li, G. F. Wang, P. L. He, W. G. Huang, F. H. Zhu, H. Y. Gao, W. Tang, Y. Luo, C. L. Feng, L. P. Shi, Y. D. Ren, W. Lu and J. P. Zuo, *J. Med. Chem.*, 2006, **49**(15), 4790–4794.
20 K. C. S. Achar, K. M. Hosamani and H. R. Seetharamareddy, *Eur. J. Med. Chem.*, 2010, **45**(5), 2048–2054.
21 C. L. Sann, A. Baron, J. Mann, H. V. D. Berg, M. Gunaratnam and S. Neidle, *Org. Biomol. Chem.*, 2006, **4**, 1305–1312.

22 T. Kálai, M. Balog, A. Szabó, G. Gulyás, J. Jeko, B. Sümegi and K. Hideg, *J. Med. Chem.*, 2009, **52**(6), 1619–1629.
23 W. W. K. R. Mederski, D. Dorsch, S. Anzali, J. Gleitz, B. Cezanne and C. Tsaklakidis, *Bioorg. Med. Chem. Lett.*, 2004, **14**, 3763–3769.
24 U. Kalinowska-Lis, A. Felczak, L. Checinska, K. Lisowska and J. Ochocki, *J. Organomet. Chem.*, 2014, **749**, 394–399.
25 X. X. Wang, Y. G. Liu, K. V. Hecke, A. Goltsev and G. H. Cui, *Z. Anorg. Allg. Chem.*, 2015, **641**(5), 903–910.
26 J. Hao, B. Yu, K. V. Hecke and G. Cui, *CrystEngComm*, 2015, **17**, 2279.
27 X. L. Lv, H. Wu, J. F. Ma and J. Yang, *Polyhedron*, 2011, **30**, 1579–1586.
28 H. L. Wu, J. K. Yuan, Y. Bai, G. L. Pan, H. Wang, J. Kong, X. Y. Fan and H. M. Liu, *Dalton Trans.*, 2012, **41**, 8829.
29 H. L. Wu, Y. H. Zhang, C. Y. Chen, J. W. Zhang, Y. C. Bai, F. R. Shi and X. L. Wang, *New J. Chem.*, 2014, **38**, 3688.
30 H. Hioki, K. Matsuhita, M. Kubo, K. Harada, M. Kodama and Y. Fukuyama, *Tetrahedron*, 2007, **63**, 11315–11324.
31 P. M. Bendale and C. M. Sun, *J. Comb. Chem.*, 2002, **4**(4), 359–361.
32 M. J. Lin and C. M. Sun, *Synlett*, 2004, 663–666.
33 M. C. Etter, *Acc. Chem. Res.*, 1990, **23**(4), 120–126.
34 A. W. Xu, C. Y. Su, Z. F. Zhang, Y. P. Cai and C. L. Chen, *New J. Chem.*, 2001, **25**, 479–482.
35 L. Yang, D. R. Powell and R. P. Houser, *Dalton Trans.*, 2007, 955–964.
36 A. W. Addison, T. N. Rao, J. Reedijk, J. van Rijn, G. C. Verschoor and J. Chem. Soc, *Dalton Trans.*, 1984, 1349–1356.
37 B. Li, W. K. Wang, S. Q. Zang and T. C. W. Mak, *J. Organomet. Chem.*, 2013, **745–746**, 173–176.
38 H. L. Wu and Y. C. Gao, *Transition Met. Chem.*, 2004, **29**(2), 175–179.
39 A. M. Pyle, J. P. Rehmann, R. Meshoyrer, C. V. Kumar, N. J. Turro and N. J. J. K. Barton, *J. Am. Chem. Soc.*, 1989, **111**, 3051–3058.
40 E. C. Long and J. K. Barton, *Acc. Chem. Res.*, 1990, **23**(9), 271–273.
41 M. Cory, D. D. McKee, J. Kagan, D. W. Henry and J. A. Miller, *J. Am. Chem. Soc.*, 1985, **107**(8), 2528–2536.
42 F. J. Meyer-Almes and D. Porschke, *Biochemistry*, 1993, **32**(16), 4246–4253.
43 Y. Wang, Z. N. ang and Z. N. Chen, *Bioorg. Med. Chem. Lett.*, 2008, **18**, 298–303.
44 J. Olmsted and D. R. Kearns, *Biochemistry*, 1977, **16**(16), 3647–3654.
45 H. Chao and L. N. Ji, *Bioinorg. Chem. Appl.*, 2005, **3**, 15–28.
46 B. Peng, H. Chao, B. Sun, H. Li, F. Gao and L. N. Ji, *J. Inorg. Biochem.*, 2007, **101**, 404–411.
47 M. Chauhan, K. Banerjee and F. Arjmand, *Inorg. Chem.*, 2007, **46**(8), 3072–3082.
48 S. Satyanarayana, J. C. Dabrowiak and J. B. Chaires, *Biochemistry*, 1992, **31**(39), 9319–9324.
49 T. M. Kelly, A. B. Tossi, D. J. McConnell and T. C. Strekas, *Nucleic Acids Res.*, 1985, **13**(17), 6017–6034.
50 P. T. Selvi and M. Palaniandavar, *Inorg. Chim. Acta*, 2002, **337**, 420–428.
51 J. Liu, H. Zhang, C. Chen, H. Deng, T. Lu and L. Ji, *Dalton Trans.*, 2003, 114–119.
52 H. L. Wu, R. R. Yun, K. T. Wang, K. Li and T. Sao, *Z. Anorg. Allg. Chem.*, 2010, **636**, 629–633.
53 Bruker, *SMART, SAINT AND SADABS*, Bruker Axs, Inc., Madison, Wisconsin, USA, 2000.
54 G. M. Sheldrick, *SHELXTL*, Siemmens Analytical X-Ray Instruments, Inc., Madison, Wisconsin, USA, 1996.
55 J. Marmur, *J. Mol. Biol.*, 1961, **3**, 208–218.
56 M. E. Reichmann, S. A. Rice, C. A. Thomas and P. Doty, *J. Am. Chem. Soc.*, 1954, **76**, 3047–3053.
57 J. R. Lakowicz and G. Webber, *Biochemistry*, 1973, **12**(21), 4161–4170.
58 S. M. Rida, F. A. Ashour, S. El-Haish, M. El-Semary, M. H. Badr and M. A. Shalaby, *Eur. J. Med. Chem.*, 2005, **40**(9), 949–959.

 